International Journal of Thermophysics, Vol. 13, No. 1, 1992

Thermodynamic Properties of Amorphous Silicon Investigated by Pulsed Laser Heating[1]

M. G. Grimaldi,[2] P. Baeri,[2] M. A. Malvezzi,[3] and C. Sirtori[3]

Nanosecond ($\lambda = 347$ nm, $\tau = 25$ ns) and picosecond ($\lambda = 532$ nm, $\tau = 20$ ps) pulsed laser irradiation have been used to induce surface melting in ion implanted and annealed amorphous silicon layers. Time-resolved reflectivity technique was employed to detect the melting onset, from which the melting temperatures of the amorphous phases have been evaluated. Thermal properties of the relaxed amorphous have also been investigated, and in particular, the differences in the heat capacity and in the thermal conductivity of the relaxed amorphous with respect to the as-implanted one were determined. Using these results, the free energy diagram of both relaxed and unrelaxed amorphous silicon has been constructed.

KEY WORDS: amorphous Si; laser irradiation; melting temperature; reflectivity; relaxation; thermal properties.

1. INTRODUCTION

Amorphous silicon has been recently shown to exist in different metastable thermodynamic states [1]: the unrelaxed one, produced by ion bombardment at temperatures below room temperature (RT), and the relaxed one obtained by thermal treatment at low temperatures (100–500°C) of the as-implanted material. The heat release during the transition between different amorphous states has been measured as a function of the annealing temperature by differential scanning calorimetry [2].

The evaluation of the thermodynamic properties of such a metastable material at high temperatures requires the use of fast temperature

[1] Paper presented at the Second Workshop on Subsecond Thermophysics, September 20–21, 1990, Torino, Italy.

[2] Dipartimento di Fisica, Università di Catania, Corso Italia 57, 95129 Catania, Italy.

[3] Dipartimento di Elettronica, Università di Pavia, Via Abbiategrasso 209, 27100 Pavia, Italy.

0195-928X/92/0100-0141$06.50/0 © 1992 Plenum Publishing Corporation

transients in order to prevent crystallization. The high heating rate obtained by nanosecond and picosecond pulsed beam irradiation allows the metastable phase to reach its melting point in a nanosecond time scale; the energy density threshold for surface melting is then directly correlated with the melting temperature of this metastable phase. The melting induced by pulsed beams has been used in the past to evaluate the melting temperature of amorphous silicon [3], of some metastable metallic alloys [4], and of Si–As supersaturated solid solutions [5]. A more precise determination of the melting temperature of ion-implanted amorphous silicon has been performed by Thompson et al. [6], who estimated $T_M = 1480 \pm 50$ K using time-resolved conductivity measurements during irradiation with nanosecond laser pulses.

The aim of this work is to investigate the changes in the heat transport properties and melting temperature induced by the relaxation process in amorphous silicon. For this purpose, we performed time-resolved reflectivity (TRR) measurements during nanosecond and picosecond laser-induced heating of amorphous silicon.

2. EXPERIMENTAL

Amorphous Si layers, 70–350 nm thick, were produced by implantation at RT of Ge^+ ions of different energies into ⟨100⟩ Si wafers. The amorphous thicknesses were measured by Rutherford backscattering spectrometry of 2.0-MeV He^+ incident along the ⟨100⟩ silicon direction. The implanted samples were subsequently vacuum annealed (residual pressure, $\sim 10^{-7}$ Torr) at 450°C for 60 min to relax the amorphous phase and to remove the damage at the crystal–amorphous interface. Part of the samples was successively derelaxed by reimplanting Ge ions at a dose ~ 0.1 the previous one [7].

Nanosecond irradiations were performed with a pulsed (25-ns FWHM) ruby laser operating at double frequency ($\lambda = 347$ nm). Lateral uniformity of the laser spot within 10% over a 3-mm-diameter circular area was achieved by means of a beam homogenizing quartz pipe. The laser spot energy density was monitored using an integrated photodiode optically coupled to the pipe. The linearity of the photodiode response within 0.3% over the entire energy density range was checked by measuring the pipe output with a high-sensitivity radiometer. Absolute calibration has not been performed in this experiment. The surface reflectivity of the irradiated sample has been probed by a 15-mW cw Ar laser beam ($\lambda = 488$ nm), π polarized, focused to a spot ~ 500 μm in diameter on the center of the pump ruby laser spot. The angle of incidence of the probe laser beam was $\sim 75°$ and the time resolution was ~ 1 ns. Care was taken

to place the irradiated samples at a distance of $600 \pm 5\ \mu m$ from the surface of the pipe output and to probe with the Ar laser the same portion of the irradiated material (within $\pm 20\ \mu m$).

Picosecond irradiations were performed using a 20-ps pulse from a doubled-frequency Nd:YAG ($\lambda = 532$ nm). Melting thresholds have been evaluated using a 20-ps, 1.064-μm pulse as probe. The probe and pump pulses were derived from the same laser, and the probe was delayed 100 ps with respect to the power pulse. The spatial profile of the laser pulses was gaussian and the ratio between the probe and the pump diameters was 1:10 in order to ensure homogeneous conditions over the sampled surface.

The TRR signals near the melting threshold exhibit a gaussian shape of constant duration. By increasing the energy density of the pump pulse, a linear increase in the reflectivity signals is observed until saturation occurs at the liquid silicon value. The transient behavior between solid and liquid silicon reflectivity results from the limited thickness of the liquid layer, which is smaller than the corresponding light extinction length in the liquid phase. Details on the behavior of the TRR signals in the near-melting threshold regime have been reported elsewhere [8].

3. PICOSECOND IRRADIATION RESULTS

In Fig. 1, the reflectivity obtained by the probe and pump method is reported versus the irradiation energy density for relaxed (upper part) and unrelaxed amorphous silicon. Near the melting threshold, the slow rise of the reflectivity-vs-energy density curve is due to the limited thickness of the molten layer since about $30\ \mathrm{mJ \cdot cm^{-2}}$ above the threshold is needed to melt a layer thicker than the absorption length at the probe wavelength in liquid Si. The threshold value, therefore, is located at the beginning of the reflectivity rise unlike, as we see in the next section, the case of nanosecond pulse irradiation.

By a fitting procedure, the ratio of the melting threshold of the relaxed a-Si to that of the unrelaxed one was found to be $E_{th}^{rel}/E_{th}^{unr} = 1.3 \pm 0.05$, where E_{th}^{rel} and E_{th}^{unr} are the threshold energy densities for surface melting of relaxed and unrelaxed a-Si, respectively.

Moreover, a partial relaxation induced by UV nanosecond laser pulses in ion-implanted a-Si has been detected by this tecnique. In fact, the melting threshold of an ion implanted a-Si sample previously heated by nanosecond laser pulses up to ~ 1000 K has been measured and found to lie between that of relaxed and that of unrelaxed a-Si. This beam-induced relaxation occurs on a nanosecond time scale and is probably related to the high photon density along the light absorption length.

In this regime, the heating process is independent of the thermal dif-

fusivity because the thermal diffusion length is much smaller than the pump penetration length during the laser pulse and the thermal conductivity does not influence the heating process. If we assume a constant value for c_p, the melting threshold is proportional to the melting temperature T_M referred to room temperature T_R:

$$E_{th} = \frac{\alpha^{-1} c_p (T_M - T_R)}{1 - R} \tag{1}$$

where c_p is the heat capacity of a-Si and α is the absorption coefficient of the irradiated sample at the laser wavelength.

The measured ratio of the relaxed a-Si melting threshold to that of the unrelaxed one can then be converted into the ratio of their melting temperatures through Eq. (1) provided that the specific heat and the optical parameters of a-Si are known.

The complex index of refraction of relaxed and unrelaxed a-Si at the pump wavelength has been determined by ellipsometric measurements;

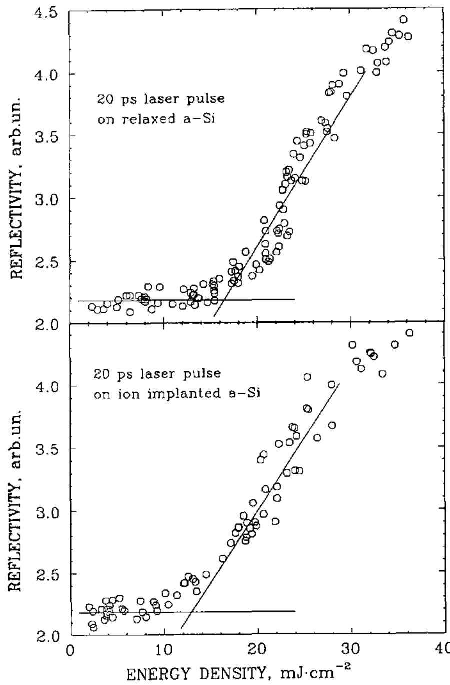

Fig. 1. Reflectivity peak signals for 1.064-μm, 30-ps pulse probe against energy density for relaxed (upper) and unrelaxed (lower) a-Si.

from this the absorption coefficient was 4×10^5 and $4.7 \times 10^5\ \mathrm{cm}^{-1}$ for relaxed and unrelaxed a-Si, respectively, while no difference was observed in the reflectivity whose value was 0.475.

4. NANOSECOND IRRADIATIONS

In order to get information on the c_p values we performed a set of experiments using UV nanosecond laser pulses to induce surface melting since in this case the heating process is strongly influenced by the heat diffusion.

4.1. Thermal Diffusivity Measurement

Ultraviolet light is absorbed in a very short distance ($\leqslant 10^{-6}$ cm) in both amorphous and crystalline silicon; the absorption length is then much smaller than the thermal diffusion length during a 30-ns laser pulse; the latter can be extimated from previous measurements of the thermal conductivity [9] and it is of the order of thousands of angstroms. In this regime, the heating of the sample can be easily modeled, and for an infinitely thick amorphous sample the heat diffusion equation can be solved analytically. The melting threshold can be calculated using the following expression:

$$(1-R)\,E_{\mathrm{th}} = \frac{\sqrt{\pi}}{2}\,(c_p \rho K)^{1/2}\,(\tau)^{1/2}\,(T_M - T_R) \qquad (2)$$

where R, c_p, ρ, K, τ, T_M, and T_R are the surface reflectance, the heat capacity, the mass density, the thermal conductivity, the duration of the laser pulse, the melting temperature, and the room temperature, respectively.

If the thickness of the amorphous layer is comparable to the thermal diffusion length during the irradiation time, then the surface heating rate and the melting threshold are strongly dependent on the thickness of the amorphous layer since the thermal conductivity of the crystalline bulk is much higher than that of the amorphous phase. In fact, the heated layer thickness during irradiation is of the order of $l = (D\tau)^{1/2}$ (where $D = K/\rho c_p$ is the thermal diffusivity) and the energy density threshold for surface melting increases with l. Because of the difference between the amorphous and the crystalline silicon thermal conductivities, a thin amorphous layer ($x_a < l$) requires a higher energy density to reach the melting temperature with respect to a thick one ($x_a > l$). In the limit of a very thick amorphous layer ($x_a \gg l$), the threshold energy density is independent of x_a. Owing to

this behavior, the thermal diffusivity of the amorphous states has been estimated performing a set of measurements of the melting threshold as a function of the amorphous layer thickness x_a.

The TRR tecnique has been used to determine the melting thresholds. Since in this experiment, unlike the picosecond case, the spatial energy inhomogeneity ($\sim 10\%$) was greater than the energy required to melt a 10-nm-thick layer (which is the absorption length at the probe wavelength), we have assumed the melting threshold to be the energy density at which the peak value of the reflectivity reaches a value halfway between that of liquid and that of solid silicon.

We have found that the melting threshold is independent of the thickness of the amorphous layer if the latter is thicker than 220 nm. The melting threshold energy density normalized to that of an infinitely thick amorphous layer (330 nm in our case) is reported as a function of thickness of the amorphous layer in Fig. 2, where circles refer to derelaxed and squares to relaxed amorphous silicon. This ratio is, to a good approximation, independent of the melting temperature of the amorphous silicon and depends only on $\sqrt{D\tau}/x_a$. The curves were calculated for different values of the thermal conductivity using the heat flow model [10] and represent the best fit to our data points. A thermal diffusivity of 2.53×10^{-3} and 1.78×10^{-3} cm^2 s^{-1} for the relaxed and unrelaxed a-Si, respectively, has been determined by the fitting procedure. This difference can result from a greater thermal conductivity and/or from a smaller heat capacity of the

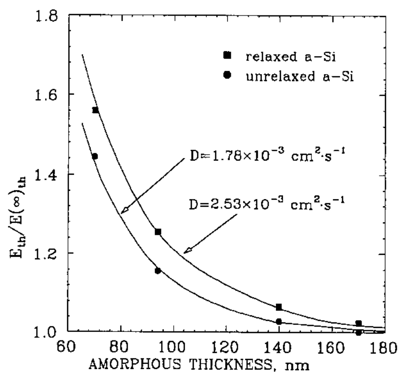

Fig. 2. Threshold energy density for surface melting normalized to that of a 330-nm-thick amorphous layer as a function of the amorphous thickness. The solid lines were calculated using the thermal model.

relaxed amorphous state with respect to the unrelaxed one. To discriminate the two contributions we performed a third experiment using nanosecond laser pulses.

4.2. Thermal Conductivity and Heat Capacity Measurement

In an infinitely thick sample, the melting threshold is proportional to the square root of the product of heat capacity and thermal conductivity [see Eq. (2)]. The variation of these parameters in amorphous silicon upon relaxation was determined by measuring the energy threshold for surface melting in a particular set of samples shown schematically in Fig. 3. Sample A: an amorphous layer 330 nm thick was obtained by implantation at RT of Ge ions at different energies (330 and 50 KeV) and doses (2×10^{15} and 4×10^{14} cm^{-2}, respectively). Sample B: a fully relaxed amorphous layer 330 nm thick was obtained by annealing sample A at 450°C for 60 min. Sample C: a thin unrelaxed amorphous layer ($\sim$17 nm) was generated at the surface of sample B by implanting 15-keV Ge ions to a dose 1×10^{14} cm^{-2}. The average concentration of the implanted Ge in the outer 10 nm was 0.04 atomic % and this causes a melting-point depression smaller than 0.1 °C.

The total thickness of the amorphous layer generated by the implantation is greater than the thermal diffusion length so that Eq. (1) can still be used. Samples A and C have exactly the same surface melting temperature but different heat flow parameters in that heat diffused through an unrelaxed (sample A) and a relaxed (sample C) amorphous layer, respectively. The thickness of the derelaxed amorphous surface layer is very small with respect to the thermal diffusion length, so that samples B and C exhibit a different surface melting temperature (if any difference exists between the relaxed and the unrelaxed amorphous states) while the heat transport and the temperature rise are determined by the thermal properties of the relaxed amorphous state. To verify this statement, we have measured the melting threshold as a function of the thickness of the unrelaxed surface layer, and a saturation of the energy density threshold

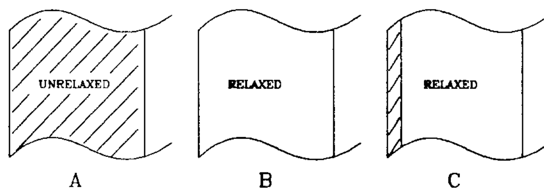

Fig. 3. Schematic description of the samples used in the experiments.

for surface melting was observed when the unrelaxed layer becomes thinner than 30 nm [11].

Any difference in the energy threshold for surface melting between sample A and sample C is to be attributed to a different heat transport toward the bulk, while any difference between sample B and sample C is indicative of a change in the melting temperature.

In Fig. 4, the peak reflectivities measured during irradiation of the samples A, B, and C are reported against the absorbed energy during the laser pulse, i.e., the photodiode output has been multiplied by $(1-R)$, where R is the reflectivity measured in our samples. The reflectivity of sample A starts to increase during irradiation at ~ 31 mV and it reaches the liquid value at ~ 39 mV. At higher energy densities, the reflectivity signals show a "plateau" typical of pulsed laser-induced melting. Samples B and C show the same behavior, the only difference being the shift of the curves toward higher energy densities. The relaxed amorphous layer (sample B) exhibits a threshold $15.9 \pm 0.3\%$ higher than the unrelaxed one (sample A). This difference is due to a change both in the melting temperature and in the thermal parameters of the amorphous silicon upon relaxation.

A comparison between the melting threshold of sample A and that of C indicates that the changes in the thermal parameters in the relaxed material can account only for a $11.7 \pm 0.2\%$ shift, while the remaining 4.2% is to be attributed to a different melting temperature.

Using Eq. (2), the above ratios indicate a 24% increase in the product Kc_p and a 3.9% increase in the melting temperature of relaxed a-Si with

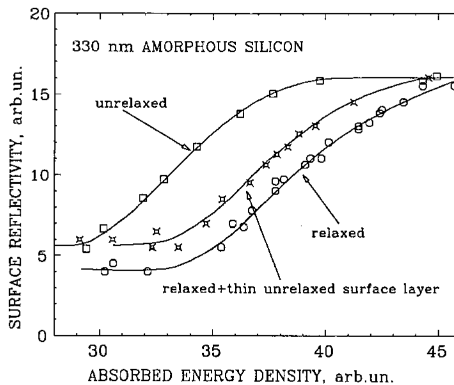

Fig. 4. Reflectivity peak signals for 488-nm laser probe during UV irradiation of samples A (□), B (○), and C (X) as a function of the energy density of the laser pulse.

respect to the unrelaxed. The increase in the product Kc_p is reliable since the measured values are representative of the thermal properties of the whole 330-nm-thick amorphous layer. However, the estimate of the increase in the melting temperature is not significant because, as we already discussed in the picosecond irradiations section, there is a beam-induced partial relaxation of the topmost 10-nm amorphous layer during irradiation with nanosecond pulses prior melting.

5. DISCUSSION AND CONCLUSION

Irradiations of relaxed and unrelaxed a-Si with ultraviolet nanosecond laser pulses have been used to obtain information on their heat capacity and thermal conductivity. This has been possible because in this regime the thermal diffusion length is greater than the light penetration depth and the heating process is strongly dependent on the thermal properties of the amorphous layer.

In our experiments, we measured both the ratio of the thermal diffusion coefficient of the relaxed a-Si D^{rel} to that of the unrelaxed one D^{unr} (see Section 4.1) to be

$$\frac{D^{\text{rel}}}{D^{\text{unr}}} = \frac{K^{\text{rel}} c_p^{\text{unr}}}{K^{\text{unr}} c_p^{\text{rel}}} = \frac{2.53}{1.78} = 1.42$$

and the ratio of the product heat capacity by thermal conductivity of relaxed a-Si to the unrelaxed one (see section 4.2) to be

$$\frac{K^{\text{rel}} c_p^{\text{rel}}}{K^{\text{unr}} c_p^{\text{unr}}} = 1.24$$

It follows that $K^{\text{rel}}/K^{\text{unr}} = 1.33$ and $c_p^{\text{unr}}/c^{\text{rel}} = 1.07$, from which the determination of the melting temperature increase in a-Si upon relaxation from the picosecond irradiation data (see Section 3) is straightforward. In fact using Eq. (1) we obtain

$$\frac{T_M^{\text{rel}} - T_R}{T_M^{\text{unr}} - T_R} \frac{\alpha^{\text{unr}} c_p^{\text{rel}}}{\alpha^{\text{rel}} c_p^{\text{unr}}} = 1.3$$

Using the previously reported data for α and assuming a melting temperature of 1480 K for the relaxed a-Si, we have calculated a melting temperature of 1320 K for the unrelaxed a-Si, i.e., we have measured ~ 150 K difference between the melting temperature of relaxed and that of unrelaxed a-Si.

Let us now compare this difference with that expected on the basis of calorimetric measurements in amorphous silicon. Based on the measurements by Donovan et al. [2], the heat release during relaxation of a-Si is ~0.25 of the total enthalpy of the amorphous phase. The relative Gibbs free energies of amorphous and liquid silicon phases referred to the crystalline phase have been calculated using those data and are reported in Fig. 5. The continous lines for the amorphous states were calculated assuming a unique value for the heat capacity:

$$c_p^{\mathrm{am.rel}}(T) - c_p^{\mathrm{xtal}}(T) = -0.224 + 4.8\,\frac{T}{1685} \qquad (\mathrm{J \cdot mol^{-1} \cdot K^{-1}})$$

We found, however, the ratio of the average heat capacity of relaxed to unrelaxed a-Si, which in turn is equivalent to write

$$c_p^{\mathrm{am.unr}}(T) - c_p^{\mathrm{xtal}}(T) = 1.6[c_p^{\mathrm{am.rel}}(T) - c_p^{\mathrm{xtal}}(T)]$$

The dashed line in Fig. 5 has been calculated using the last expression for $c_p^{\mathrm{am.unr}}$. The difference between the melting temperature of relaxed and that of unrelaxed a-Si calculated from Fig. 5 is ~200 K if we assume a unique heat capacity for the amorphous states, while it reduces to ~150 K if we use the heat capacities we have measured for the two amorphous states. The last estimate is in excellent agreement with the melting temperature difference determined by picosecond laser irradiation.

A final remark can be made on our interpretation of the experimental data based on the assumption of temperature-independent K and c_p parameters, which allowed us to use approximate analytical solutions of

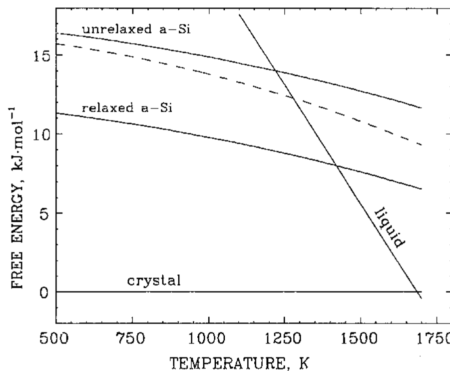

Fig. 5. Relative Gibbs free energy of amorphous and liquid silicon phases referred to the crystal phase versus temperature.

the heat flow equation. In Ref. 12 a complete analysis which takes into account the temperature dependence of all thermal and optical parameters by numerical solution of the heat flow equation has been reported, and it has been shown that equivalent results are obtained if one uses constant thermal parameters whose value is an average between room temperature and the melting temperature.

REFERENCES

1. S. Roorda, S. Doorn, W. C. Sinke, P. M. Scholte, and E. van Loenen, *Phys. Rev. Lett.* **62**:1880 (1989).
2. E. P. Donovan, F. Spaepen, J. M. Poate, and D. C. Jacobson, *Appl. Phys. Lett.* **55**:1516 (1989).
3. P. Baeri, G. Foti, J. M. Poate, and A. G. Cullis, *Phys. Rev. Lett.* **45**:2036 (1980).
4. J. A. Knapp and D. M. Follstaed, *Phys. Rev. Lett.* **58**:2454 (1987).
5. P. Baeri, R. Reitano, A. M. Malvezzi, and A. Borghesi, *J. Appl. Phys.* **67**:1801 (1990).
6. M. O. Thompson, G. J. Galvin, J. W. Mayer, P. S. Peercy, J. M. Poate, D. C. Jacobson, A. G. Cullis, and N. G. Chew, *Phys. Rev. Lett.* **52**:2360 (1984).
7. S. Roorda, W. C. Sinke, J. M. Poate, D. C. Jacobson, S. Dierker, B. S. Dennis, D. J. Eaglesham, and F. Spaepen, *Mat. Res. Soc. Symp. Proc.* **157**:709 (1990).
8. G. E. Jellison, D. H. Lowndes, D. N. Mashburn, and R. F. Wood, *Phys. Rev. B* **34**:2407 (1986).
9. M. G. Grimaldi, P. Baeri, and G. Baratta, *Mat. Res. Soc. Symp. Proc.* **157**:419 (1990).
10. P. Baeri and S. U. Campisano, in *Laser Annealing of Semiconductors*, J. M. Poate and J. W. Mayer, eds. (Academic Press, New York, 1982), pp. 77–109.
11. M. G. Grimaldi and P. Baeri, *Appl. Phys. Lett.* **57**:614 (1990).
12. M. G. Grimaldi, P. Baeri, and M. A. Malvezzi, *Phys. Rev. B* (in press).